Cofilin-1 and profilin-1 expression in lung microvascular endothelial cells exposed to titanium dioxide nanoparticles

Min-Hyeok An[A–E], Seon-Muk Choi[B–E], Pureun-Haneul Lee[A–C,E], Shinhee Park[A–C], Ae Rin Baek[A–C], An-Soo Jang[A–F]

Department of Internal Medicine, Soonchunhyang University Bucheon Hospital, South Korea

A – research concept and design; B – collection and/or assembly of data; C – data analysis and interpretation;
D – writing the article; E – critical revision of the article; F – final approval of the article

Advances in Clinical and Experimental Medicine, ISSN 1899–5276 (print), ISSN 2451–2680 (online) *Adv Clin Exp Med*. 2022;31(11):1255–1264

Address for correspondence
An-Soo Jang
E-mail: jas877@schmc.ac.kr

Funding sources
None declared

Conflict of interest
None declared

Acknowledgements
This research received the support of the Basic Science Research Program through the National Research Foundation of Korea (NRF) funded by the Ministry of Science, ICT and Soonchunhyang University (grant No. NRF-2020R1A2C1006506).

Received on November 16, 2021
Reviewed on March 15, 2022
Accepted on July 11, 2022

Published online on August 24, 2022

Abstract

Background. Air pollutants exacerbate chronic airway diseases, such as asthma and chronic obstructive pulmonary disease (COPD). However, the underlying mechanisms are yet to be determined. While a number of studies have reported adverse effects of nanoparticles on humans, little is known about their effects on the respiratory system.

Objectives. To examine the protein expression in human lung microvascular endothelial cells (HMVEC-L) exposed to titanium dioxide (TiO_2) nanoparticles, a common air pollutant.

Materials and methods. A proteomics approach using two-dimensional polyacrylamide gel electrophoresis (2D-PAGE) and matrix-assisted laser desorption/ionization time-of-flight/time-of-flight mass spectrometry (MALDI-TOF/TOF MS) was used to determine the differences in protein expression at 8 h and 24 h, following the treatment of HMVEC-L with 20-μM or 40-μM TiO_2 nanoparticles.

Results. Human lung microvascular endothelial cells treated with 20-μM TiO_2 nanoparticles showed alterations of 7 protein spots, including molecules related to calcium regulation, transport, cytoskeleton, and muscle contraction. The treatment of HMVEC-L with 40-μM TiO_2 nanoparticles resulted in alterations of 4 protein spots, with molecular functions related to the cytoskeleton, myosin regulation, actin modulation, as well as guanosine diphosphate (GDP) and guanosine triphosphate (GTP) regulation. To validate these results, immunohistochemical staining and western blotting analyses were performed on lung tissues collected from mice exposed to TiO_2 nanoparticles. Cofilin-1 and profilin-1 were expressed in the endothelium, epithelium and inflammatory cells, and decreased in lung tissues of TiO_2 nanoparticle-exposed mice compared to sham-treated controls.

Conclusions. These results suggest that some of the differentially expressed proteins may play important roles in airway diseases caused by TiO_2 nanoparticle exposure.

Key words: proteomics, air pollutants, airway disease, nanoparticles

Cite as
An MH, Choi SM, Lee PH, Park S, Baek AR, Jang AS. Cofilin-1 and profilin-1 expression in lung microvascular endothelial cells exposed to titanium dioxide nanoparticles. *Adv Clin Exp Med*. 2022;31(11):1255–1264. doi:10.17219/acem/152032

DOI
10.17219/acem/152032

Background

Air pollutants encompass also toxic particles and gases emitted in large quantities from many different sources, including vehicles and factories.[1] Major pollutants include particulate matter (PM), ozone, nitrogen dioxide (NO_2), and sulfur dioxide (SO_2). Air pollution negatively impacts human health and increases the burden of disease and demand for healthcare services.[2–4]

The principal component of indoor and outdoor air pollution is PM, which can vary widely in particle size, and includes coarse, fine and ultrafine particles. Furthermore, PM is a complex mixture of materials with a carbonaceous core and associated materials, such as organic compounds, acids and fine metal particles.[5,6]

Inflammation exacerbates pulmonary disease and causes lung dysfunction. The most important issue regarding environmental air pollution is its toxic effect, which can result in inflammatory disease,[7,8] with the lung function of patients with airway disease showing greater deterioration among those living in communities exposed to high levels of air pollution.[9] Toxic titanium dioxide (TiO_2) nanoparticles are produced by human activities, such as driving automobiles and charcoal burning, as well as by natural processes.[10–12] Titanium dioxide nanoparticles have toxic effects that manifest in inflammation and lead to disease.[13–15] Furthermore, the exposure to TiO_2 nanoparticles induces both acute and chronic inflammation, increases inflammatory cell expression and mucosal gland hyperplasia in the airway and alveolar spaces in animal models,[13,16,17] and can cause itching, bronchoconstriction and mucus hypersecretion.[18] The TiO_2 nanoparticles achieve this by penetrating the cell membrane and exerting toxic effects in organs.[19,20] Our previous studies demonstrated that the exposure to TiO_2 nanoparticles induced pulmonary inflammation and activated the inflammasome in mice, causing differential expression of NLRP3, caspase-1, and cytokines IL-1β and IL-18 in the lungs.[5] Moreover, TiO_2 nanoparticles increase the production of reactive oxygen species (ROS) and oxidative products, as well as the depletion of cellular antioxidants.[21,22]

Tight junctions (TJs) are the apical-most constituents of the junctional complex in epithelial cell sheets, also present in vascular endothelial cells and mesothelial cells.[22] Tight junctions act as a semipermeable barrier to the paracellular transport of ions, solutes and water, and function as a barrier between the apical and basolateral domains of plasma membranes.[22] Tight junctions coordinate a variety of signaling and trafficking molecules involved in the regulation of cell differentiation, proliferation and polarity, and thereby serve as multifunctional complexes.[21,23] The disruption of the function of TJs can cause or contribute to a variety of pathological conditions, such as infections, cancers and blood-borne metastasis.[24] Endothelial cells are among the main cellular constituents of blood vessels, and one of their most important functions is the formation of a barrier between blood and underlying tissues. These endothelial junctional proteins play important roles in tissue integrity, vascular permeability, leukocyte extravasation, and angiogenesis.[21]

The actin-severing activity of cofilin is an important factor in the stretch-induced cytoskeletal fluidization and may account for an appreciable part of the bronchodilatory effects of a deep inspiration.[28] Both cigarette smoke-exposed and chronic obstructive pulmonary disease (COPD) patient-derived epithelia display quantitative evidence of cellular plasticity, along with a loss of specialized apical features with distinct cell motion indicative of cellular jamming. These injured/diseased cells have an increased fraction of polymerized actin, due to the loss of the actin-severing protein, cofilin-1.[29] Counteracting cofilin-1 is profilin-1, an actin-binding protein that promotes actin polymerization in vitro,[25,26] endothelial cell migration and proliferation.[27] A requirement for dynamic actin association and dissociation is rendered by reversible Ser^{71} phosphorylation and dephosphorylation. The phosphorylation of Ser^{71} inhibits actin-binding of profilin-1.[30]

The mechanisms by which toxic nanoparticles induce pulmonary disease remain to be elucidated. In this study, we examined whether nanoparticles play a role in lung disease employing two-dimensional polyacrylamide gel electrophoresis (2D-PAGE) and matrix-assisted laser desorption/ionization time-of-flight/time-of-flight mass spectrometry (MALDI-TOF/TOF MS) of endothelial cells, and examined protein expression in the lungs of a mouse model of asthma.

Objectives

This study investigated whether TiO_2 nanoparticle exposure altered protein expression in vitro and in vivo.

Materials and methods

Cell culture and stimulation with TiO_2 nanoparticles

Primary human lung microvascular endothelial cells (HMVEC-L; 5000 cells/cm^2, cat No. CC-2527; Lonza, Basel, Switzerland) were grown in EGM™-2MV Microvascular Endothelial Cell Growth Medium BulletKit™ (Lonza). The medium was replaced every 48 h until cells reached 90% confluence at 37°C in 5% CO_2. The cells were seeded in 6-well plates. Twenty-four hours before the experiment, the medium was changed to EBM-2 supplemented with 0.1% fetal bovine serum (FBS). After 30 min, cells were stimulated with TiO_2 nanoparticles (SRM 1898, 20 or 40 μM; National Institute of Standards & Technology (NIST), Gaithersburg, USA) for 8 h or 24 h. The endotoxin concentration in nanoparticles was <0.064 ng/mL (0.32 EU/mL), based on the limulus amebocyte lysate assay (QCL-1000; BioWhittaker, Walkersville, USA).

Two-dimensional electrophoresis and image analysis

Human lung microvascular endothelial cells were harvested by centrifugation and then disrupted with lysis buffer containing 5 mM Tris-HCl (pH 7.4), 100 mM NaCl, 1% Triton X-100 and 2 mM phenylmethylsulfonyl fluoride (PMSF). Cell lysates were centrifuged at 12,000 rpm for 30 min and the supernatant was collected. The protein concentration was determined using a commercial BCA assay kit (Thermo Fisher Scientific, Rockford, USA) and the samples were stored at –70°C until use. Immobiline DryStrips (Amersham Biosciences, Piscataway, USA) were used for isoelectric focusing (IEF), which was carried out with 1 mg of the protein on an IPGphor system (Amersham Biosciences). The proteins were then separated in the second dimension by sodium dodecyl sulfate (SDS)-PAGE. Staining was performed with Coomassie brilliant blue G250 for the visualization of proteins. The 2-D gels were scanned with an ImageScanner (Amersham Biosciences) in a transmission mode. Spot detection and matching were performed using ImageMaster 2D v. 5.0 (Amersham Biosciences). The 2D spot intensity was calculated by integrating the optical density over the spot area. The data normalization was performed using ImageMaster 2D v. 5.0 (GE Healthcare, Seoul, South Korea) and then the values were exported to SPSS software v. 18.0 (SPSS Inc., Chicago, USA) for statistical analysis.

Protein identification with MALDI-TOF/TOF MS

Mass spectrometry was performed at Yonsei Proteome Research Center (YPRC; Seoul, South Korea). Synovial fluid and serum peptide profiles were analyzed with a MALDI-TOF/TOF mass spectrometer (Micromass, Wilmslow, UK). The following reagents and solutions were used for sample preparation: 70% acetonitrile (ACN), 2% formaldehyde and 2% fluorescent antibody (FA) buffer. Finally, the peptides attached to the resin were eluted in a drop-by-drop manner using an elution buffer.

Database search and protein identification

Peptide matching and protein searches against the Swiss-Prot and NCBI databases were performed using the Mascot software (Matrix Science; http://www.matrixscience.com).

Animal experiment

All experimental protocols were approved by the Animal Care and Use Committee of Soonchunhyang University, Asan, South Korea (approval No. SCHBCA-2015-06).[31] Six-week-old female BALB/c mice (n = 8 per group) were sensitized by intraperitoneal (ip.) injection on days 0 and 14, with grade V chicken egg ovalbumin (OVA, 50 μg; Sigma-Aldrich, St. Louis, USA) emulsified in 10 mg of $Al(OH)_3$ plus Dulbecco's phosphate-buffered saline (D-PBS, 100 μL). On days 21–23, all mice received an intranasal challenge with grade III OVA (150 μg; Sigma-Aldrich) in D-PBS (50 μL). Control mice were sensitized and challenged with saline. In the TiO_2 nanoparticle groups, mice were exposed to TiO_2 nanoparticles by inhalation (200 $\mu g/m^3$ for 2 h) before OVA challenge, every day for 3 days. The airway hyperresponsiveness was measured on day 23. Bronchoalveolar lavage fluid (BALF) and lung tissues of mice were then collected for further analysis, including measurement of cofilin-1 and profilin-1 in lung protein, as well as BALF.

Determination of airway responsiveness and morphological analysis

Mice were challenged with 0 mg/mL (baseline), 5 mg/mL, 20 mg/mL, or 100 mg/mL methacholine. After challenge, enhanced pause (Penh) was measured using methacholine in a barometric plethysmographic chamber (All Medicus Co., Anyang, South Korea). Mice were anesthetized the next day and BALF was obtained and stored at –20°C until use. Differential cell counts within BALF samples were determined with Diff-Quick staining of cytospin slides (500 cells per animal). A portion of the lung was fixed in 4% buffered paraformaldehyde and embedded in paraffin. The tissue was cut into 4-μm-thick sections for histological analysis. The images were captured using an ECLIPSE Ci-L microscope (Nikon Corp., Tokyo, Japan) equipped with a DS-Ri2 digital camera (Nikon Corp.).

Western blotting analysis

The extracted lung tissue was homogenized in protein lysis solution containing 50 mM Tris-HCl (pH 7.4), 50 mM NaCl, 0.1% SDS, 1% TritonX-100, 0.5 mM ethylenediaminetetraacetic acid (EDTA), and 100 mM PMSF in distilled water, and centrifuged at 14,000 rpm for 30 min at 4°C. Then, the soluble fraction was collected. Mouse lung proteins were separated with SDS-PAGE and transferred onto polyvinylidene difluoride (PVDF) membranes, which were then blocked with 5% bovine serum albumin (BSA) plus 0.1% Tween 20 in Tris-buffered saline (TBS) for 2 h at room temperature. The membranes were incubated with rabbit anti-cofilin-1 (1:5000; Abcam, Cambridge, UK), mouse anti-profilin-1 (1:100; Santa Cruz Biotechnology, Santa Cruz, USA) or rabbit anti-profilin-1 (1:1000; ECM Biosciences, Versailles, USA) antibody overnight at 4°C. The next day, the membranes were incubated with horseradish peroxidase (HRP)-conjugated secondary antibodies. The detection was performed using EzWestLumi plus western blot detection reagent (ATTO Corporation, Tokyo, Japan). The relative abundances of the proteins were determined using quantitative densitometry with normalization relative to β-actin (Sigma-Aldrich).

Immunohistochemistry

Mouse lung sections were deparaffinized and rehydrated by passage through a series of increasing concentrations of ethanol. The sections were treated with 1.4% H_2O_2 in methanol for 30 min to block endogenous peroxidase activity, and nonspecific binding was then blocked with 1.5% normal horse serum. Next, the samples were incubated with rabbit anti-cofilin-1 (1:2000; Abcam) or mouse anti-profilin-1 (1:50; Santa Cruz Biotechnology) antibody. The next day, the sections were incubated using an ABC kit (Vector Laboratories, Burlingame, USA), and the color reaction was developed by staining with a DAB substrate kit (Golden Bridge International Inc., Mukilteo, USA). After immunohistochemical staining, the slides were counterstained with Harris hematoxylin for 1 min. Staining was quantified using ImageJ software (National Institutes of Health (NIH), Bethesda, USA).

Statistical analyses

The researchers hypothesized that the TiO_2 affects asthma pathogenesis through regulating cofilin-1 and profilin-1. Alternatively, a null hypothesis was proposed by the researchers, which advocated that there was no statistically significant difference between the groups. The data were expressed as median and interquartile range (IQR). All data were analyzed using IBM SPSS v. 22.0 software (IBM Corp., Armonk, USA). The differences between groups were determined using the nonparametric Kruskal–Wallis test, followed by Dunn's post hoc test. A value of $p < 0.05$ was considered statistically significant.

Results

2D-PAGE of HMVEC-L exposed to TiO_2 nanoparticles

A proteomics approach was used to determine the differential expression of proteins 8 h and 24 h after treating HMVEC-L with 20- or 40-μM TiO_2 nanoparticles (Fig. 1). A total of 11 spots were detected on each gel, all identified spots were localized in the 3–10 pH range, and the molecular mass ranged from 10 kDa to 150 kDa.

Protein spots selected on 2D-PAGE

Following the treatment for 8 h or 24 h with TiO_2 nanoparticles, 7 and 4 spots were found to have a differential, greater than two-fold expression on 2D-PAGE gel extracts (concentrations of 20 μM and 40 μM, respectively). These spots were excised from the gel and incubated with trypsin to digest the proteins in the gel, and then analyzed using MALDI-TOF/TOF MS (Table 1).

Identification of protein in each spot

Moesin, calreticulin precursor, eukaryotic initiation factor 4A-I isoform 1, heat shock protein β-1, profilin-1, myosin light polypeptide 6, and chain A were identified in the spots showing a differential expression. The differential expression (up or down) was shown in the Table 1 (average at 8 h and 24 h) on exposure to TiO_2 nanoparticles at a concentration of 20 μM. Furthermore, changes

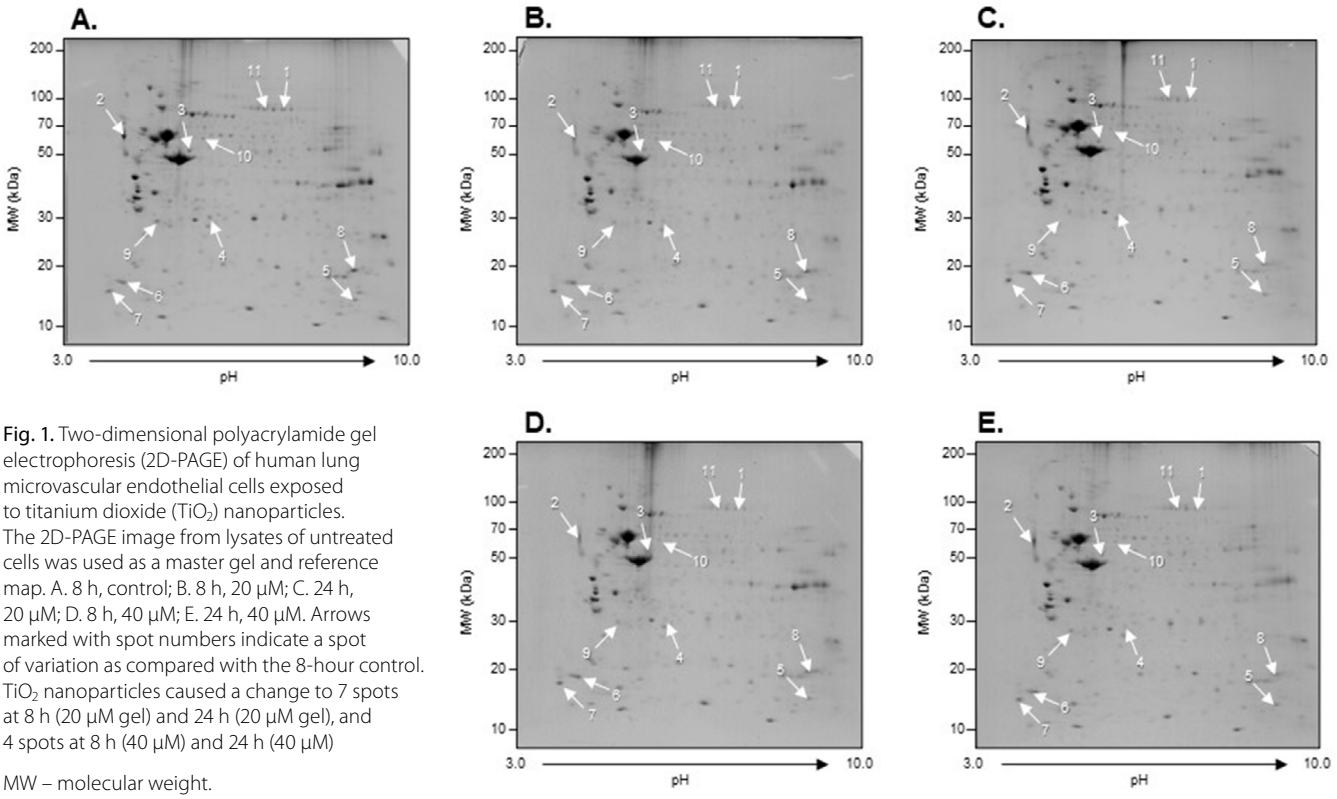

Fig. 1. Two-dimensional polyacrylamide gel electrophoresis (2D-PAGE) of human lung microvascular endothelial cells exposed to titanium dioxide (TiO_2) nanoparticles. The 2D-PAGE image from lysates of untreated cells was used as a master gel and reference map. A. 8 h, control; B. 8 h, 20 μM; C. 24 h, 20 μM; D. 8 h, 40 μM; E. 24 h, 40 μM. Arrows marked with spot numbers indicate a spot of variation as compared with the 8-hour control. TiO_2 nanoparticles caused a change to 7 spots at 8 h (20 μM gel) and 24 h (20 μM gel), and 4 spots at 8 h (40 μM) and 24 h (40 μM)

MW – molecular weight.

Table 1. List of proteins identified using matrix-assisted laser desorption/ionization time-of-flight/time-of-flight mass spectrometry (MALDI-TOF/TOF MS)

No.	TiO_2 NPs	Protein	Functional categorization	Accession number	Amino acid sequence	pI/molecular mass [Da]	Sequence coverage [%]	Average ratio (8 h)	Average ratio (24 h)
1.	concentration: 20 μM	moesin	cytoskeleton	4505257	K.VTAQDVR.K	6.08/67892	34	−2.59	−2.12
2.		calreticulin precursor	Ca^{2+} regulation	45757900	K.NVLINK.D	4.29/48283	17	−2.27	−1.72
3.		eukaryotic initiation factor 4A-I isoform 1	initiation factor	4503529	R.ENYIHR.I	5.32/46353	31	−3.37	−2.58
4.		heat shock protein β-1	cytoskeleton	4504517	R.VPFSLLR.G	5.98/22826	28	−1.83	2.54
5.		Profilin-1	transport	4826898	K.TLVLLMGK.E	8.44/15216	26	−3.21	2.89
6.		myosin light polypeptide 6 isoform	muscle contraction	17986258	K.SDEMNVK.V	4.56/17090	38	−1.34	1.85
7.		chain A target enzyme recognition by calmodulin	Ca^{2+} regulation	640285	K.ELGTVMR.S	4.04/16568	6	1.96	2.68
8.	concentration: 40 μM	cofilin-1	actin modulation	5031635	K.VFNDMK.V	8.22/18719	34	−3.04	2.5
9.		rho GDP-dissociation inhibitor 1 isoform A	regulation GDP/GTP	4757768	K.EGVEYR.I	5.02/23250	16	−2.32	2.83
10.		cytokeratin 7	cytoskeleton	67782365	R.LEAELR.S	5.40/51411	36	−1.8	2.31
11.		glycyl-tRNA synthetase	protein coding	578814645	R.AEFLNK.S	6.18/62596	11	−2.41	2.19

NPs – nanoparticles; GDP/GTP – guanosine diphosphate/guanosine triphosphate; pI – isoelectric point.

in the expression of cofilin-1, rho GDP-dissociation inhibitor 1 isoform A, cytokeratin 7, and glycyl-tRNA synthetase were detected in cells exposed to 40-μM TiO_2 nanoparticles. The identified spots had biological functions related to the cytoskeleton, calcium regulation, initiation factors, transport, muscle contraction, actin modulation, guanosine diphosphate/guanosine triphosphate (GDP/GTP) regulation, and protein coding.

Airway hyperresponsiveness and inflammatory changes on exposure to OVA and OVA plus TiO_2 nanoparticles

Airway hyperresponsiveness and inflammatory cells were increased in mice exposed to OVA and TiO_2 nanoparticles, compared to sham-treated control mice. Moreover, the increase was more pronounced with OVA+TiO_2 nanoparticles compared to OVA alone (Fig. 2, Table 2,3).

Protein validation with western blotting and immunohistochemical analyses

Western blotting analysis revealed decreases in cofilin-1 and profilin-1 expressions in HMVEC-L exposed to TiO_2 nanoparticles for 24 h, but not in cells exposed for 8 h (Fig. 3A, Table 4,5). Furthermore, there were no changes in protein expression after 8 h or 24 h of starving the cells. The expression of profilin-1 was increased by exposure to TiO_2 nanoparticles in a time-dependent manner (Fig. 3A, Table 4,5). The expression levels of cofilin-1 and profilin-1 were increased in lung tissue of asthmatic mice compared to control mice and were decreased in the OVA+TiO_2 nanoparticles group compared to the OVA group (Fig. 3B, Table 2,3). The level of profilin-1 was significantly decreased in the sham-treated group, but it was increased in both the OVA group and the TiO_2 groups (Fig. 3B, Table 2,3). The immunohistochemical analysis indicated that cofilin-1 and profilin-1 levels in lung tissue were increased in the OVA group compared to the control group, but the increase was less pronounced in the OVA+TiO_2 nanoparticles group (Fig. 4, Table 2,3).

Discussion

This study revealed changes in protein expression in endothelial cells exposed to TiO_2 nanoparticles using a proteomics approach. Cofilin-1 and profilin-1 were shown to contribute to airway inflammation in the lungs of mice exposed to these potent air pollutants.

Ambient pollution has both a particulate component and a gaseous component, with the major fractions relevant

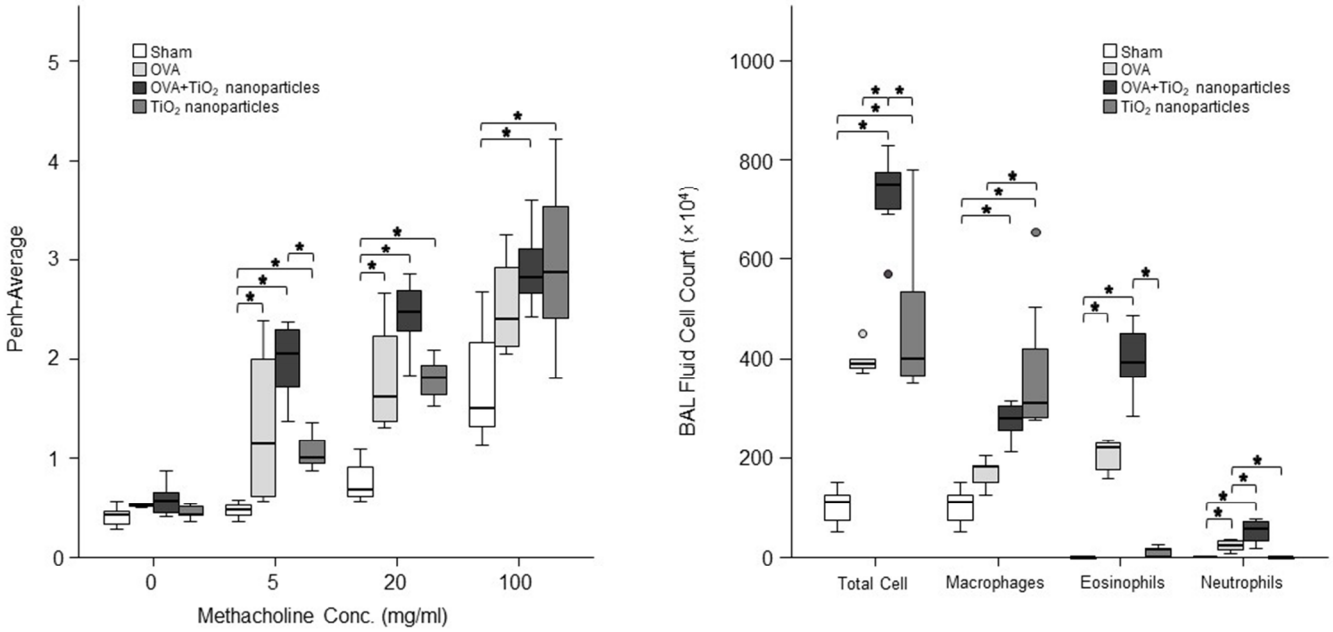

Fig. 2. Airway hyperresponsiveness and airway inflammation changes in a mouse ovalbumin (OVA)/titanium dioxide (TiO_2) nanoparticle-treated model. A. Airway hyperresponsiveness in OVA/TiO_2 nanoparticle-treated mice; B. Differential inflammatory cell counts in the bronchoalveolar lavage fluid (BALF) of OVA/TiO_2 nanoparticle-treated mice. The data are presented as median (interquartile range (IQR)) of 8 mice per group (* $p < 0.05$ compared with the sham group)

Table 2. Comparison of the analyzed variables in titanium dioxide (TiO_2) nanoparticle-exposed mice model profile using Kruskal–Wallis test (median, interquartile range (IQR))

Variable	Groups				Kruskal–Wallis test	
	group A (sham)	group B (OVA)	group C (OVA+TiO_2)	group D (TiO_2)	χ^2	p-value
AHR						
Mch 0 mg/mL	0.42 (0.33–0.47)	0.53 (0.51–0.56)	0.57 (0.43–0.67)	0.43 (0.41–0.52)	9.273	0.095
Mch 5 mg/mL	0.48 (0.43–0.53)	0.67 (0.59-2.00)	2.05 (1.59–2.32)	1.00 (0.91–1.24)	20.125	<0.001*
Mch 20 mg/mL	0.68 (0.62–0.97)	1.79 (1.37–2.33)	2.48 (2.23–2.77)	1.74 (1.55–1.97)	20.494	<0.001*
Mch 100 mg/mL	1.51 (1.32–2.29)	2.58 (2.13–3.09)	2.82 (2.63–3.16)	2.79 (1.88–3.63)	12.755	0.005*
Diff (×10⁴)						
Total cells	110 (60–130)	390 (375–425)	750 (695–777.5)	400 (357.5–592.5)	19.131	<0.001*
Macrophages	109.78 (59.64–129.48)	181.74 (138.16–194.56)	278.81 (255.63–307.575)	309.57 (278.58–461.76)	16.661	0.001*
Eosinophils	0.36 (0–0.52)	220.5 (167.56–233.23)	390.03 (360.405–451.9)	15.38 (2.355–18.345)	24.042	<0.001*
Neutrophils	0 (0–0)	23.4 (11.67–34.23)	55.9 (31–73.005)	0 (0–0.82)	23.531	<0.001*
Lymphocytes	0 (0–0)	0.9 (0.38–1.94)	0 (0–0)	0 (0–0)	20.547	<0.001*
WB (intensity) (protein:b-actin ratio)						
Cofilin	0.659 (0.385–1.036)	1.166 (0.851–1.692)	0.663 (0.335–0.942)	0.332 (0.184–0.793)	9.353	0.025*
Profilin	0.7 (0.629–0.889)	1.055 (0.97–1.252)	0.859 (0.625–1.111)	0.577 (0.317–0.727)	10.393	0.016*
Profilin-1	0.588 (0.424–0.761)	0.357 (0.333–0.407)	0.49 (0.384–0.55)	1.592 (1.464–1.669)	17.42	0.001*
IHC (intensity [%])						
Cofilin	8.22 (7.625–10.546)	21.374 (18.246–24.895)	13.888 (11.559–16.773)	5.822 (4.063–7.805)	13.5	0.004*
Profilin	9.205 (8.204–11.887)	26.578 (15.872–30.421)	15.129 (12.401–18.199)	8.022 (6.378–10.439)	11.713	0.008*

AHR – airway hyperresponsiveness; Mch – methacholine; Diff – different cell count; WB – western blot; IHC – immunohistochemistry; OVA – ovalbumin; $p > 0.05$: non-significant, * $p < 0.05$: significant.

to health designated as PM_{10} (10 μm), $PM_{2.5}$ (2.5 μm) and ultrafine PM.[32] Moreover, air pollution causes and exacerbates asthma, as demonstrated in a meta-analysis that revealed the associations between the exposure to traffic-related pollutants (black carbon, NO), $PM_{2.5}$ and PM_{10}, and the development of asthma in children.[32] Meta-analyses of the associations between air pollution and asthma exacerbations requiring emergency healthcare

Table 3. The p-values of Dunn's post hoc test comparisons for variables between the titanium dioxide (TiO_2) nanoparticle-exposed mice groups

Groups						
Variable	A vs B	A vs C	A vs D	B vs C	B vs D	C vs D
AHR						
Mch 0 mg/mL	–	–	–	–	–	–
Mch 5 mg/mL	0.017*	<0.001*	0.022*	0.217	0.651	0.045*
Mch 20 mg/mL	0.04*	<0.001*	0.011*	0.105	0.92	0.073
Mch 100 mg/mL	0.123	0.002*	0.003*	0.304	0.336	0.958
Diff ($\times 10^4$)						
Total cells	0.074	<0.001*	0.029*	0.034*	0.879	0.024*
Macrophages	0.27	0.002*	<0.001*	0.082	0.03*	0.627
Eosinophils	0.006*	<0.001*	0.166	0.165	0.122	0.001*
Neutrophils	0.007*	<0.001*	0.491	0.279	0.031*	<0.001*
Lymphocytes	<0.001	1	1	<0.001	<0.001	1
WB (intensity) (protein:b-actin ratio)						
Cofilin	0.111	0.744	0.153	0.003*	0.055	0.27
Profilin	0.041*	0.488	0.27	0.178	0.002*	0.072
Profilin-1	0.037*	0.462	0.045*	0.178	<0.001*	0.006*
IHC (intensity [%])						
Cofilin	0.012*	0.181	0.373	0.235	0.001*	0.026*
Profilin	0.017*	0.119	0.504	0.414	0.002*	0.026*

AHR – airway hyperresponsiveness; Mch – methacholine; Diff – different cell count; WB – western blot; IHC – immunohistochemistry; OVA – ovalbumin; $p > 0.05$: non-significant, $p < 0.05$: significant*. Groups (A: sham, B: OVA, C: OVA+TiO_2, D: TiO_2). The Kruskal–Wallis test and the Dunn's post hoc test were used.

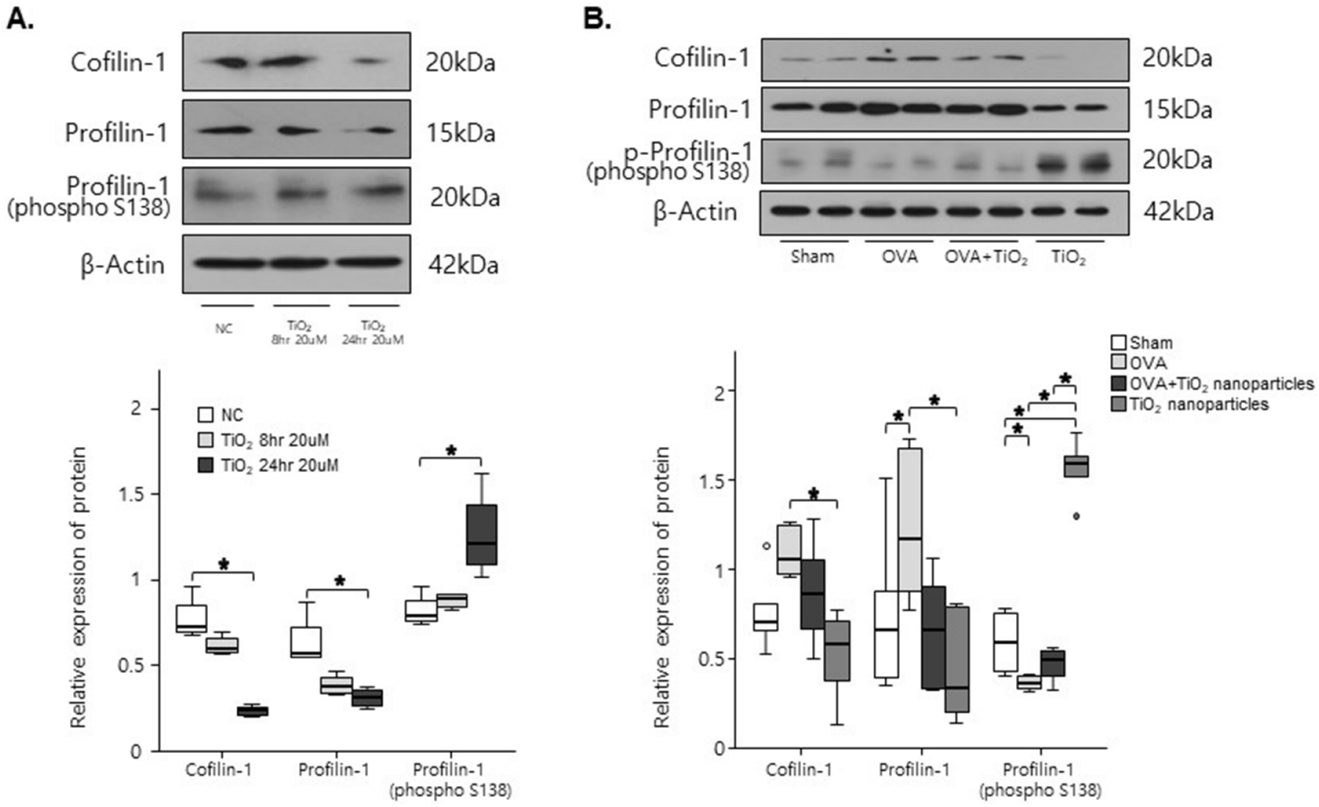

Fig. 3. The expression levels of cofilin-1 and profilin-1 proteins dected with western blotting. A. Cofilin-1 and profilin-1 levels in human lung microvascular endothelial cells (HMVEC-L) exposed to 20-μM TiO_2 nanoparticles for 8 h or 24 h (* $p < 0.05$ compared to normal controls (NC)); B. Cofilin-1 and profilin-1 levels determined with western blotting in ovalbumin (OVA)/titanium dioxide (TiO_2) nanoparticle-treated mice. The band intensities of cofilin-1 and profilin-1 were compared to that of β-actin. The data presented as the median (interquartile range (IQR)) of 8 mice per group (* $p < 0.05$ compared with the sham group)

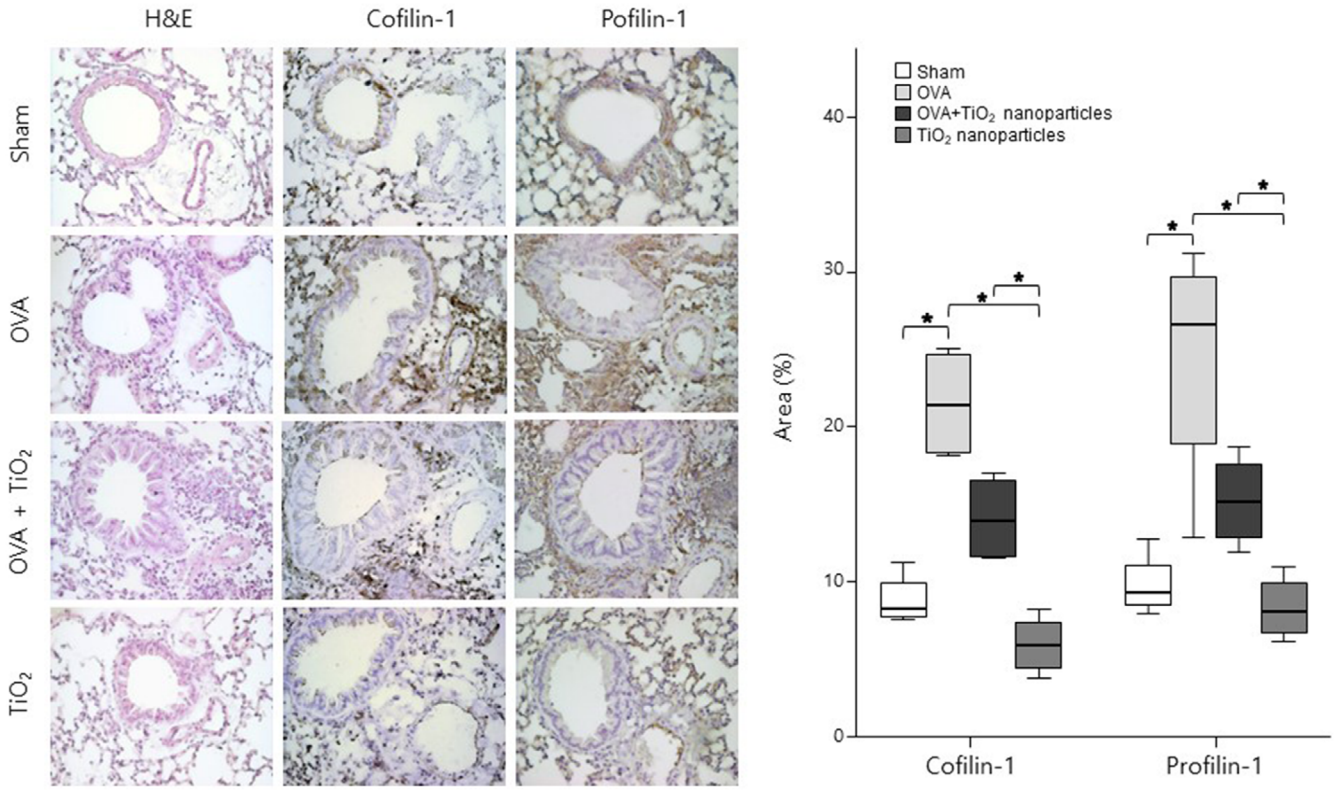

Fig. 4. Lung tissue cofilin-1 and profilin-1 protein expression visualized using hematoxylin and eosin (H&E) and immunohistochemical stain in ovalbumin (OVA)/titanium dioxide (TiO_2) nanoparticle-treated and sham mice

* $p < 0.05$ compared with the sham group.

Table 4. Comparison of the analyzed variables in 20-μM titanium dioxide (TiO_2) nanoparticle-exposed human lung microvascular endothelial cells (HMVEC-L) profile using Kruskal–Wallis test (median, interquartile range (IQR))

Variable	Groups			Kruskal–Wallis test	
	group A (NC)	group B (8 h)	group C (24 h)	χ^2	p-value
WB (intensity) (protein:b-actin ratio)					
Cofilin	0.727 (0.689–0.904)	0.596 (0.572–0.676)	0.236 (0.206–0.267)	9.269	0.01*
Profilin	0.566 (0.55–0.795)	0.374 (0.336–0.448)	0.309 (0.257–0.369)	8.346	0.015*
Profilin-1	0.791 (0.75–0.922)	0.886 (0.836–0.916)	1.209 (1.054–1.53)	8	0.018*

WB – western blot; $p > 0.05$: non-significant, $p < 0.05$: significant*; NC – normal controls.

Table 5. The p-values of Dunn's post hoc test comparisons for variables between the 20-μM titanium dioxide (TiO_2) nanoparticle-exposed human lung microvascular endothelial cells (HMVEC-L) groups

Variable	Groups		
	A vs B	A vs C	B vs C
WB (intensity) (protein:b-actin ratio)			
Cofilin	0.17	0.002*	0.096
Profilin	0.062	0.004*	0.327
Profilin-1	0.433	0.006*	0.05

WB – western blot; $p > 0.05$: non-significant, $p < 0.05$: significant*. Groups (A: NC – normal controls. B: TiO_2 exposed 8 h, C: TiO_2 exposed 24 h). The Kruskal–Wallis test and the Dunn's post hoc test were used.

utilization in children and/or adults also showed significant associations for NO_2, $PM_{2.5}$, CO, and O_3.[33,34]

Particulate matter with a diameter smaller than 100 nm is defined as ultrafine particles or nanoparticles. Nanoparticles are mainly found in urban air as single and aggregated particles, and can be divided into 2 major categories based on their source. Typically, nanoparticles are generated incidentally, often as byproducts of fossil fuel combustion and condensation

of semi-volatile substances or industrial emissions, although they can also be produced through engineering processes.[19,35] The exposure to PM induces oxidative stress and inflammation, stimulating both the innate and acquired immune responses in laboratory animals and humans. Oxidant-mediated cellular damage, including the production of ROS and oxidative stress, and innate and adaptive immunity, can lead to PM-mediated adverse health effects.[19]

Our previous studies showed that air pollutants promote lung disease through various mechanisms, including innate immunity (e.g., via macrophage migration inhibitory factor and inflammasomes) and neuroinflammation.[8,31,36] Nanoparticles also alter lung structure, reflected in goblet cell hyperplasia and airway remodeling.[13,37]

In this study, proteomic analyses showed that the treatment of HMVEC-L with 20-μM TiO_2 nanoparticles altered the expression of 7 proteins, including moesin, calreticulin precursor, eukaryotic factor 4A-isoform 1, heat shock protein β-1, profilin-1, myosin light polypeptide 6, and chain A, while the treatment with 40-μM TiO_2 nanoparticles altered the expression of 4 proteins, including cofilin-1, rho GDP-dissociation inhibitor 1 isoform A, cytokeratin 7, and glycyl-tRNA synthetase, that have roles in calcium regulation, transport, cytoskeleton, muscle contraction, myosin regulation, actin modulation, and GDP and GTP regulation.[38,39] Further studies are needed to clarify the role of this variety of expressed proteins in air pollutant-induced lung diseases.

Cofilin is a widely distributed intracellular actin-modulating protein that binds and depolymerizes filamentous (F)-actin and inhibits the polymerization of monomeric globular (G)-actin in a pH-dependent manner. It is involved in the translocation of actin-cofilin complex from the cytoplasm to the nucleus.[39] Cofilin modulates actin transport and function in the nucleus as well as actin organization associated with mitochondrial fission and mitophagy. Cofilin-saturated F-actin fragments under stress conditions can undergo oxidative cross-linking and bundle together to form cofilin-actin rods.[41] Cofilin-1 is a part of a novel mechanism linking mechano-transduction and transcription.[42] Profilin-1 is a 140-amino acid protein that regulates the growth of F-actin by binding to monomeric G-actin.[38] In the present study, cofilin-1 and profilin-1 protein expression levels were changed in endothelial cells and lungs exposed to TiO_2 nanoparticles, suggesting that these proteins may be useful markers of nanoparticle exposure in the lung. These results can be partly explained by recent experiments.[40–42] Injured epithelial cells exposed to cigarette smoke in COPD have an increased fraction of polymerized actin, due to loss of the actin-severing protein cofilin-1.[40] Further studies are needed to clarify the underlying signaling pathways and implications of these findings for airway diseases.

The respiratory epithelia function as a selective barrier between the outside environment and underlying tissue. Tight junctions are considered to function as a barrier between the apical and basolateral domains of plasma membranes.[21,43] In this study, TiO_2 nanoparticles altered the lung structure and disrupted the function of TJs in epithelial cells and endothelial cells, suggesting that nanoparticles can penetrate cell barriers and promote airway inflammation and hyperresponsiveness, thus contributing to airway remodeling.

Limitations

Future studies are needed for the multi-omics approaches which would lead to a more comprehensive overview, as compared to single-omics layer with slight advantages for combinations that complement each other directly, e.g., proteome and metabolome.[44–47]

Conclusions

In conclusion, nanoparticles are involved in airway inflammation and responsiveness (mediated by cofilin-1 and profilin-1), and in the change of cell membranes. Further studies are necessary to determine the mechanisms underlying these effects.

ORCID iDs

Min-Hyeok An https://orcid.org/0000-0002-7058-1870
Seon-Muk Choi https://orcid.org/0000-0003-4831-049X
Pureun-Haneul Lee https://orcid.org/0000-0002-1431-2393
Shinhee Park https://orcid.org/0000-0002-5783-6795
Ae Rin Baek https://orcid.org/0000-0003-1350-610X
An-Soo Jang https://orcid.org/0000-0001-5343-023X

References

1. McCormack MC, Breysse PN, Hansel NN, et al. Common household activities are associated with elevated particulate matter concentrations in bedrooms of inner-city Baltimore pre-school children. *Environ Res*. 2008;106(2):148–155. doi:10.1016/j.envres.2007.08.012
2. Murray CJL, Aravkin AY, Zheng P, et al. Global burden of 87 risk factors in 204 countries and territories, 1990–2019: A systematic analysis for the Global Burden of Disease Study 2019. *Lancet*. 2020;396(10258):1223–1249. doi:10.1016/S0140-6736(20)30752-2
3. Lee PH, Park S, Lee YG, Choi SM, An MH, Jang AS. The impact of environmental pollutants on barrier dysfunction in respiratory disease. *Allergy Asthma Immunol Res*. 2021;13(6):850–862. doi:10.4168/aair.2021.13.6.850
4. Leikauf GD, Kim SH, Jang AS. Mechanisms of ultrafine particle-induced respiratory health effects. *Exp Mol Med*. 2020;52(3):329–337. doi:10.1038/s12276-020-0394-0
5. Chipps BE, Murphy KR, Oppenheimer J. 2020 NAEPP Guidelines Update and GINA 2021: Asthma care differences, overlap, and challenges. *J Allergy Clin Immunol Pract*. 2022;10(1):S19–S30. doi:10.1016/j.jaip.2021.10.032
6. Stojanovic N, Glisovic J, Abdullah OI, Belhocine A, Grujic I. Particle formation due to brake wear, influence on the people health and measures for their reduction: A review. *Environ Sci Pollut Res*. 2022;29(7):9606–9625. doi:10.1007/s11356-021-17907-3
7. Müzes G, Sipos F. Inflammasome, inflammation and cancer: An interrelated pathobiological triad. *Curr Drug Targets*. 2015;16(3):249–257. doi:10.2174/1389450115666141229154157
8. Kim BG, Lee PH, Lee SH, Park MK, Jang AS. Effect of TiO_2 nanoparticles on inflammasome-mediated airway inflammation and responsiveness. *Allergy Asthma Immunol Res*. 2017;9(3):257–264. doi:10.4168/aair.2017.9.3.257

9. Decrue F, Gorlanova O, Salem Y, et al. Increased impact of air pollution on lung function in preterm versus term infants: The BILD study. *Am J Respir Crit Care Med*. 2022;205(1):99–107. doi:10.1164/rccm.202102-0272OC
10. Guo C, Yu T, Bo Y, et al. Long-term exposure to fine particulate matter and mortality: A longitudinal cohort study of 400,459 adults. *Epidemiology*. 2022;33(3):309–317. doi:10.1097/EDE.0000000000001464
11. Grande F, Tucci P. Titanium dioxide nanoparticles: A risk for human health? *Mini Rev Med Chem*. 2016;16(9):762–769. doi:10.2174/1389557516666160321114341
12. Iswarya V, Palanivel A, Chandrasekaran N, Mukherjee A. Toxic effect of different types of titanium dioxide nanoparticles on *Ceriodaphnia dubia* in a freshwater system. *Environ Sci Pollut Res*. 2019;26(12):11998–12013. doi:10.1007/s11356-019-04652-x
13. Meldrum K, Guo C, Marczylo EL, Gant TW, Smith R, Leonard MO. Mechanistic insight into the impact of nanomaterials on asthma and allergic airway disease. *Part Fibre Toxicol*. 2017;14(1):45. doi:10.1186/s12989-017-0228-y
14. Meyer TJ, Scherzad A, Moratin H, et al. The radiosensitizing effect of zinc oxide nanoparticles in sub-cytotoxic dosing is associated with oxidative stress in vitro. *Materials (Basel)*. 2019;12(24):4062. doi:10.3390/ma12244062
15. Feltis BN, Elbaz A, Wright PFA, Mackay GA, Turney TW, Lopata AL. Characterizing the inhibitory action of zinc oxide nanoparticles on allergic-type mast cell activation. *Mol Immunol*. 2015;66(2):139–146. doi:10.1016/j.molimm.2015.02.021
16. Korábková E, Kašpárková V, Jasenská D, et al. Behaviour of titanium dioxide particles in artificial body fluids and human blood plasma. *Int J Mol Sci*. 2021;22(19):10614. doi:10.3390/ijms221910614
17. Kang CM, Jang AS, Ahn MH, et al. Interleukin-25 and interleukin-13 production by alveolar macrophages in response to particles. *Am J Respir Cell Mol Biol*. 2005;33(3):290–296. doi:10.1165/rcmb.2005-0003OC
18. Sarasola M de la P, Táquez Delgado MA, Nicoud MB, Medina VA. Histamine in cancer immunology and immunotherapy: Current status and new perspectives. *Pharmacol Res Perspect*. 2021;9(5):e00778. doi:10.1002/prp2.778
19. Leikauf GD, Kim SH, Jang AS. Mechanisms of ultrafine particle-induced respiratory health effects. *Exp Mol Med*. 2020;52(3):329–337. doi:10.1038/s12276-020-0394-0
20. Lee YG, Lee PH, Choi SM, An MH, Jang AS. Effects of air pollutants on airway diseases. *Int J Environ Res Public Health*. 2021;18(18):9905. doi:10.3390/ijerph18189905
21. Lee PH, Park S, Lee YG, Choi SM, An MH, Jang AS. The impact of environmental pollutants on barrier dysfunction in respiratory disease. *Allergy Asthma Immunol Res*. 2021;13(6):850–862. doi:10.4168/aair.2021.13.6.850
22. Wang Y, Rezey AC, Wang R, Tang DD. Role and regulation of Abelson tyrosine kinase in Crk-associated substrate/profilin-1 interaction and airway smooth muscle contraction. *Respir Res*. 2018;19(1):4. doi:10.1186/s12931-017-0709-4
23. Sugimoto K, Chiba H. The claudin–transcription factor signaling pathway. *Tissue Barriers*. 2021;9(3):1908109. doi:10.1080/21688370.2021.1908109
24. Nur Husna SM, Tan HTT, Md Shukri N, Mohd Ashari NS, Wong KK. Nasal epithelial barrier integrity and tight junctions disruption in allergic rhinitis: Overview and pathogenic insights. *Front Immunol*. 2021;12:663626. doi:10.3389/fimmu.2021.663626
25. Yang C, Huang M, DeBiasio J, et al. Profilin enhances Cdc42-induced nucleation of actin polymerization. *J Cell Biol*. 2000;150(5):1001–1012. doi:10.1083/jcb.150.5.1001
26. Porta JC, Borgstahl GEO. Structural basis for profilin-mediated actin nucleotide exchange. *J Mol Biol*. 2012;418(1–2):103–116. doi:10.1016/j.jmb.2012.02.012
27. Ding Z, Lambrechts A, Parepally M, Roy P. Silencing profilin-1 inhibits endothelial cell proliferation, migration and cord morphogenesis. *J Cell Sci*. 2006;119(Pt 19):4127–4137. doi:10.1242/jcs.03178
28. Lan B, Krishnan R, Park CY, et al. Transient stretch induces cytoskeletal fluidization through the severing action of cofilin. *Am J Physiol Lung Cell Mol Physiol*. 2018;314(5):L799–L807. doi:10.1152/ajplung.00326.2017
29. Ghosh B, Nishida K, Chandrala L, et al. Epithelial plasticity in COPD results in cellular unjamming due to an increase in polymerized actin. *J Cell Sci*. 2022;135(4):jcs258513. doi:10.1242/jcs.258513
30. Wang F, Zhu C, Cai S, et al. Ser71 phosphorylation inhibits actin-binding of profilin-1 and its apoptosis-sensitizing activity. *Front Cell Dev Biol*. 2021;9:692269. doi:10.3389/fcell.2021.692269
31. Kim BG, Park MK, Lee PH, et al. Effects of nanoparticles on neuroinflammation in a mouse model of asthma. *Respir Physiol Neurobiol*. 2020;271:103292. doi:10.1016/j.resp.2019.103292
32. Kelly FJ, Fussell JC. Air pollution and public health: Emerging hazards and improved understanding of risk. *Environ Geochem Health*. 2015;37(4):631–649. doi:10.1007/s10653-015-9720-1
33. Khreis H, Kelly C, Tate J, Parslow R, Lucas K, Nieuwenhuijsen M. Exposure to traffic-related air pollution and risk of development of childhood asthma: A systematic review and meta-analysis. *Environ Int*. 2017;100:1–31. doi:10.1016/j.envint.2016.11.012
34. Orellano P, Quaranta N, Reynoso J, Balbi B, Vasquez J. Effect of outdoor air pollution on asthma exacerbations in children and adults: Systematic review and multilevel meta-analysis. *PLoS One*. 2017;12(3):e0174050. doi:10.1371/journal.pone.0174050
35. Orach J, Rider CF, Carlsten C. Concentration-dependent health effects of air pollution in controlled human exposures. *Environ Int*. 2021;150:106424. doi:10.1016/j.envint.2021.106424
36. Cha MH, Rhim T, Kim KH, Jang AS, Paik YK, Park CS. Proteomic identification of macrophage migration-inhibitory factor upon exposure to TiO_2 particles. *Mol Cell Proteomics*. 2007;6(1):56–63. doi:10.1074/mcp.M600234-MCP200
37. Kim BG, Lee PH, Lee SH, et al. Long-term effects of diesel exhaust particles on airway inflammation and remodeling in a mouse model. *Allergy Asthma Immunol Res*. 2016;8(3):246–256. doi:10.4168/aair.2016.8.3.246
38. Pandey DK, Chaudhary B. Evolutionary expansion and structural functionalism of the ancient family of profilin proteins. *Gene*. 2017;626:70–86. doi:10.1016/j.gene.2017.05.024
39. Chang CY, Leu JD, Lee YJ. The actin depolymerizing factor (ADF)/cofilin signaling pathway and DNA damage responses in cancer. *Int J Mol Sci*. 2015;16(2):4095–4120. doi:10.3390/ijms16024095
40. Ghosh B, Nishida K, Chandrala L, et al. Epithelial plasticity in COPD results in cellular unjamming due to an increase in polymerized actin. *J Cell Sci*. 2022;135(4):jcs258513. doi:10.1242/jcs.258513
41. Bamburg JR, Minamide LS, Wiggan O, Tahtamouni LH, Kuhn TB. Cofilin and actin dynamics: Multiple modes of regulation and their impacts in neuronal development and degeneration. *Cells*. 2021;10(10):2726. doi:10.3390/cells10102726
42. Domingues C, Geraldo AM, Anjo SI, et al. Cofilin-1 is a mechanosensitive regulator of transcription. *Front Cell Dev Biol*. 2020;8:678. doi:10.3389/fcell.2020.00678
43. Zihni C, Mills C, Matter K, Balda MS. Tight junctions: From simple barriers to multifunctional molecular gates. *Nat Rev Mol Cell Biol*. 2016;17(9):564–580. doi:10.1038/nrm.2016.80
44. Karkossa I, Raps S, von Bergen M, Schubert K. Systematic review of multi-omics approaches to investigate toxicological effects in macrophages. *Int J Mol Sci*. 2020;21(24):9371. doi:10.3390/ijms21249371
45. Bannuscher A, Karkossa I, Buhs S, et al. A multi-omics approach reveals mechanisms of nanomaterial toxicity and structure–activity relationships in alveolar macrophages. *Nanotoxicology*. 2020;14(2):181–195. doi:10.1080/17435390.2019.1684592
46. Bannuscher A, Hellack B, Bahl A, et al. Metabolomics profiling to investigate nanomaterial toxicity in vitro and in vivo. *Nanotoxicology*. 2020;14(6):807–826. doi:10.1080/17435390.2020.1764123
47. Karkossa I, Bannuscher A, Hellack B, et al. An in-depth multi-omics analysis in RLE-6TN rat alveolar epithelial cells allows for nanomaterial categorization. *Part Fibre Toxicol*. 2019;16(1):38. doi:10.1186/s12989-019-0321-5